J. Astrophys. Astr. (2015) **36,** 399–407

Discovery of a Faint Eclipsing Binary GSC 02265-01456

D. F. Guo[1], K. Li[1,2,*], S. M. Hu[1], Y. G. Jiang[1], D. Y. Gao[1] & X. Chen[1]
[1]*Shandong Provincial Key Laboratory of Optical Astronomy and Solar-Terrestrial Environment, Institute of Space Sciences, Shandong University, Weihai 264209, China.*
[2]*Key Laboratory for the Structure and Evolution of Celestial Objects, Chinese Academy of Sciences, Beijing, China.*
[*]*e-mail: likai@ynao.ac.cn*

Received 18 May 2015; accepted 3 August 2015

Abstract. When observing the transiting extrasolar planets, we found a new eclipsing binary named GSC 02265-01456. The V and R_c observations were carried out for this binary. The photometric light curves of the two bands were simultaneously analyzed using the W–D code. The solutions show that GSC 02265-01456 is an extremely low mass ratio ($q = 0.087$) overcontact binary system with a contact degree of $f = 82.5\%$. The difference between the two maxima of the light curve can be explained by a dark spot on the primary component.

Key words. Stars: binaries: close—stars: binaries: eclipsing—stars: individual: GSC 02265-01456.

1. Introduction

Eclipsing binaries have historically played an important role in studying stellar astrophysics. This type of system can provide fundamental mass and radius measurements for both components, based on high-quality radial velocity curves and photometric light curves. The mass and radius measurements can accordingly test stellar evolution models (e.g., Pols *et al.* 1997; Guinan *et al.* 2000; Torres & Ribas 2002). At the same time, the luminosities for both components of these systems can be computed from the absolute radii and effective temperatures. This in turn allows for distance determinations. Indeed, they are widely used to determine distances to globular clusters and extragalactic systems (Bonanos *et al.* 2003; North *et al.* 2010; Kaluzny *et al.* 2013).

In this context, we carried out a program on searching eclipsing binaries from historical observations such as the blazars observations and the transiting extrasolar planets. We have discovered two eclipsing binaries (GSC 03517-00663 and GSC 03553-00845) for this program (Guo *et al.* 2014, 2015). In this paper, we present another newly identified eclipsing binary GSC 02265-01456 ($\alpha_{2000} = 00^h20^m15^s.03$, $\delta_{2000} = +31°58'22''.9$) which was discovered when observing the

transiting extrasolar planet WASP-1b. The V and R_c light curve observation and investigation are presented in sections 2 and 3. The results are discussed in section 4.

2. Observations and results

When analyzing the observational data directed toward the study of transiting extrasolar planets (WASP-1b), one of the field stars was detected varying more than 0.1 magnitudes (V band) on the night of November 8, 2008. Neither the GCVS nor the NSV catalogues contain this star, so we concluded that it is a new variable star. This star was named GSC 02265-01456 based on the GSC 1.2. The galactic longitude and latitude coordinates are $l = +115°15'41''.8$ and $b = -30°26'01''.7$, respectively.

In order to identify the type of this variable star, subsequent CCD photometric observations of GSC 02265-01456 were carried out using an Andor DZ936 CCD camera attached to the 1.0-m Cassegrain telescope at Weihai Observatory of Shandong University, on October 16 and November 14, 2014. Detailed information of the telescope can be found in Hu *et al.* (2014). The Andor DZ936 camera has 2048×2048 square pixels (13.5×13.5 μm pixel^{-1}), providing an effective field-of-view of about $12' \times 12'$. The standard Johnson and Cousins V, and R_c filters were used during our observations. The typical integration times for each image were 120 s and 90 s in V and R_c bands, respectively. The reductions of observations were performed using the APPHOT packages in IRAF procedures.[1] All data were processed by bias and flat-field correction. A nearby star with similar brightness and similar color (GSC 02265-00144) was used as a comparison star to minimize the influence of differential extinction. One of the CCD images is shown in Figure 1, where V refers to the variable star (i.e., GSC 02265-01456), C (GSC 02265-00144, $\alpha_{2000.0} = 0^h20^m16.99^s$, $\delta_{2000.0} = 31°57'53.06''$) to the comparison star, and CH (GSC 02265-00580, $\alpha_{2000.0} = 0^h20^m15.2^s$, $\delta_{2000.0} = 31°59'03.9''$) to the check star. The data for V and R_c bands are listed in Tables 1 and 2, respectively.

Jurkevich method (Jurkevich 1971) was adopted for periodicity analysis using all the V band data spanning 6 years. Given that the Jurkevich method is based on the expected mean square deviation and the unevenly spaced observations, it is less inclined to produce a fictitious periodicity when compared with a Fourier analysis. It involves testing a series of trial periods and the data are folded based on the trial periods. All data are divided into m groups in accordance with their phases around each trial period. Then the variance V_i^2 for each group and the sum of each group variance V_m^2 are calculated. If a trial period equals the authentic one, V_m^2 would reach its minimum. The results derived by the Jurkevich method using $m = 50$ are shown in the left panel of Figure 2. The minimum value implies the period of 0.355578 days.

For comparing and further investigating the reliability of the period, the software PDM13 (Zalian *et al.* 2014) based on the phase dispersion minimization technique was used to analyze the periodicity. The details and strategies of the PDM13 can be found in Zalian *et al.* (2014). Running PDM13 on GSC 02265-01456, a frequency of

[1] IRAF is distributed by the National Optical Astronomy Observatories, which is operated by the Association of Universities for Research in Astronomy Inc., under contract to the National Science Foundation.

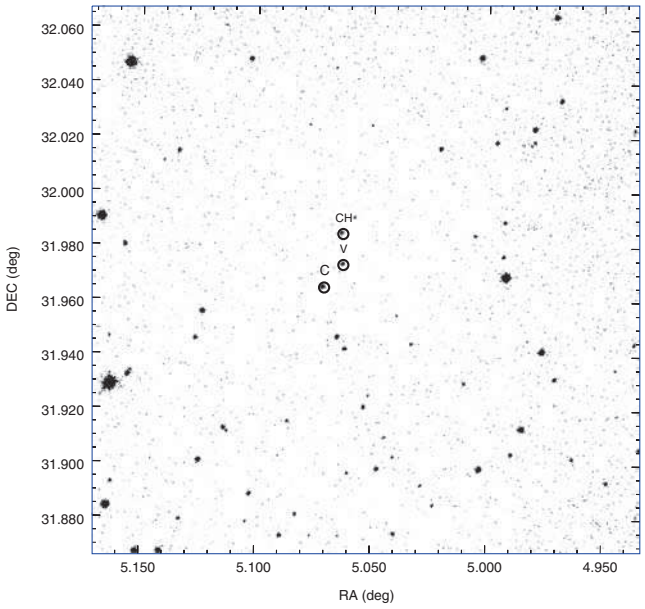

Figure 1. CCD image in the field-of-view around GSC 02265-01456. *V* refers to the variable star (i.e., GSC 02265-01456), *C* to the comparison star, and *CH* to the check star. The field-of-view is about $12' \times 12'$. North is up and east is to the left.

$f = 2.812321227d^{-1}$ was derived (see the right panel of Figure 2), corresponding to 0.355578 days, which is consistent with the period obtained by Jurkevich method.

All the observations in the V band and the newly observed V and R_c band light curves are folded based on the following ephemeris:

$$\text{Min.I} = \text{HJD2456976.0503}(\pm 0.0007) + 0.355578(\pm 0.000001)E, \qquad (1)$$

and they are displayed in the left and right panel of Figure 3, respectively.

3. Light curve investigation

The V and R_c light curve analysis of GSC 02265-01456 was started using the Wilson–Devinney (W–D) code (Wilson & Devinney 1971; Wilson 1990, 1994). From NOMAD (The Naval Observatory Merged Observatory Merged Astrometric Dataset, Zacharias *et al.* 2004), GSC 02265-01456 's color index was determined to be $B - V = 0.25$. Based on the NASA/IPAC Extragalactic Database (NED), we found that the $E(B - V)$ is 0.0502 ± 0.0025 (the uncertainty was estimated according to Schlafly & Finkbeiner 2011). Then, the $(B - V)_0$ of GSC 02265-01456 was derived to be 0.20. Therefore, the effective temperature of primary component of GSC 02265-01456 was set to be $T_1 = 7900$ according to Cox (2000). The gravity-darkening coefficient and the bolometric albedo of the primary component were taken to be $g_1 = 1$ and $A_1 = 1$ based on Lucy (1967) and Ruciński (1969). Bolometric and bandpass limb-darkening parameters were derived from Van Hamme (1993).

Table 1. V-band CCD observations for GSC 02265-01456.

JD(Hel.) 2456900+	Δm	JD(Hel.) 2456900+	Δm	JD(Hel.) 2456900+	Δm	JD(Hel.) 2456900+	Δm
46.93686	1.341	47.04398	1.320	47.15800	1.320	47.31278	1.295
46.93961	1.346	47.04948	1.304	47.16075	1.304	47.31553	1.286
46.94236	1.306	47.05222	1.312	47.16350	1.312	47.31828	1.309
46.94511	1.317	47.05497	1.322	47.16625	1.322	47.32103	1.291
46.94786	1.330	47.05772	1.333	47.16900	1.333	47.32378	1.282
46.95061	1.330	47.06047	1.325	47.17175	1.325	47.32653	1.279
46.95336	1.324	47.06322	1.330	47.17450	1.330	47.32927	1.287
46.95611	1.298	47.06597	1.325	47.17725	1.325	47.33202	1.300
46.95886	1.304	47.06872	1.325	47.17999	1.325	76.00527	1.371
46.96161	1.299	47.07147	1.352	47.18274	1.352	76.00807	1.363
46.96435	1.275	47.07422	1.337	47.18549	1.337	76.01087	1.385
46.96710	1.290	47.07971	1.338	47.18824	1.338	76.01367	1.377
46.96985	1.299	47.08246	1.367	47.19085	1.367	76.01651	1.392
46.97260	1.277	47.08521	1.344	47.19360	1.344	76.01936	1.402
46.97535	1.274	47.08796	1.360	47.19634	1.360	76.02221	1.414
46.97810	1.299	47.09071	1.365	47.19909	1.365	76.02505	1.412
46.98085	1.295	47.09350	1.367	47.20184	1.367	76.02790	1.408
46.98360	1.277	47.09635	1.370	47.20459	1.370	76.03079	1.419
46.98635	1.297	47.09919	1.384	47.20734	1.384	76.03363	1.418
46.98910	1.312	47.10203	1.395	47.21009	1.395	76.03648	1.444
46.99185	1.304	47.10487	1.401	47.21284	1.401	76.03928	1.434
46.99460	1.304	47.10771	1.424	47.25517	1.424	76.04212	1.426
46.99734	1.296	47.11055	1.414	47.26341	1.414	76.04497	1.452
47.00000	1.294	47.11339	1.391	47.26880	1.391	76.04781	1.447
47.00274	1.327	47.11624	1.389	47.27155	1.389	76.05065	1.444
47.00549	1.333	47.11906	1.391	47.27429	1.391	76.05346	1.443
47.00824	1.322	47.12190	1.384	47.27704	1.384	76.05626	1.437
47.01099	1.350	47.12474	1.382	47.27979	1.382	76.05901	1.420
47.01374	1.345	47.12758	1.355	47.28254	1.355	76.06177	1.419
47.01649	1.342	47.13038	1.352	47.28529	1.352	76.06457	1.413
47.01924	1.357	47.13322	1.350	47.28804	1.350	76.06732	1.427
47.02199	1.352	47.13597	1.354	47.29079	1.354	76.07008	1.409
47.02474	1.351	47.13877	1.344	47.29354	1.344	76.07283	1.414
47.02748	1.357	47.14156	1.337	47.29629	1.337	76.07558	1.385
47.03023	1.378	47.14431	1.325	47.29904	1.325	76.07834	1.393
47.03298	1.380	47.14711	1.331	47.30179	1.331	76.08109	1.398
47.03573	1.381	47.14985	1.317	47.30453	1.317	76.08385	1.377
47.03848	1.393	47.15260	1.306	47.30728	1.306	76.08660	1.386
47.04123	1.411	47.15535	1.333	47.31003	1.333	76.08936	1.364

These parameters of the secondary component could be determined based on the effective temperature of the secondary component.

The W–D program was started with mode 2, corresponding to a detached system. However, the two components are always filling the inner Roche lobe. Then, mode 3 was used to determine the photometric elements. During the solutions, the adjustable parameters are: the inclination i, the effective temperature of secondary component, T_2, the monochromatic luminosity of the primary component, L_{1V} and L_{1R_c}, and the dimensionless potentials of the two component, $\Omega_1 = \Omega_2$.

Since GSC 02265-01456 is a newly discovered eclipsing binary, we conducted an extensive q-search to determine the mass ratio, meaning that we calculated a series

Table 2. R_c-band CCD observations for GSC 02265-01456.

JD(Hel.) 2456900+	Δm	JD(Hel.) 2456900+	Δm	JD(Hel.) 2456900+	Δm	JD(Hel.) 2456900+	Δm
46.93828	1.200	47.04540	1.277	47.15402	1.188	47.30870	1.205
46.94103	1.200	47.04814	1.286	47.15666	1.174	47.31145	1.163
46.94378	1.191	47.05089	1.286	47.15942	1.190	47.31420	1.173
46.94653	1.212	47.05364	1.296	47.16217	1.186	47.31695	1.199
46.94928	1.203	47.05639	1.297	47.16492	1.194	47.31970	1.163
46.95203	1.200	47.05914	1.290	47.16767	1.200	47.32245	1.183
46.95478	1.173	47.06189	1.292	47.17042	1.196	47.32519	1.199
46.95753	1.173	47.06464	1.292	47.17316	1.190	47.32794	1.174
46.96028	1.170	47.06739	1.294	47.17591	1.207	47.33069	1.165
46.96302	1.178	47.07014	1.301	47.17866	1.210	47.33344	1.179
46.96577	1.199	47.07288	1.300	47.18141	1.208	76.00674	1.220
46.96852	1.175	47.07563	1.281	47.18416	1.214	76.00954	1.237
46.97127	1.179	47.07838	1.284	47.18691	1.215	76.01233	1.254
46.97402	1.172	47.08113	1.303	47.18954	1.225	76.01513	1.261
46.97677	1.166	47.08388	1.296	47.19226	1.224	76.01798	1.258
46.97952	1.194	47.08663	1.293	47.19501	1.226	76.02083	1.272
46.98227	1.169	47.08938	1.281	47.19776	1.240	76.02368	1.264
46.98502	1.154	47.09217	1.279	47.20051	1.248	76.02652	1.261
46.98777	1.181	47.09497	1.278	47.20326	1.254	76.02936	1.281
46.99051	1.173	47.09781	1.275	47.20601	1.247	76.03510	1.317
46.99326	1.184	47.10065	1.263	47.20876	1.252	76.03795	1.317
46.99601	1.185	47.10349	1.252	47.21151	1.284	76.04075	1.309
46.99865	1.180	47.10633	1.264	47.26208	1.290	76.04359	1.308
47.00141	1.190	47.10918	1.239	47.26483	1.284	76.04644	1.316
47.00416	1.196	47.11202	1.246	47.26747	1.269	76.04928	1.324
47.00691	1.213	47.11486	1.229	47.27021	1.261	76.05212	1.338
47.00966	1.202	47.11770	1.240	47.27296	1.263	76.05493	1.320
47.01241	1.187	47.12052	1.237	47.27571	1.274	76.05768	1.311
47.01516	1.215	47.12336	1.240	47.27846	1.268	76.06043	1.317
47.01791	1.223	47.12621	1.228	47.28121	1.260	76.06323	1.306
47.02066	1.214	47.12905	1.216	47.28396	1.256	76.06599	1.297
47.02340	1.225	47.13184	1.214	47.28671	1.237	76.06874	1.307
47.02615	1.238	47.13464	1.214	47.28946	1.226	76.07150	1.296
47.02890	1.250	47.13743	1.181	47.29221	1.203	76.07425	1.266
47.03165	1.270	47.14023	1.195	47.29496	1.228	76.07701	1.274
47.03440	1.259	47.14298	1.195	47.29771	1.204	76.07976	1.275
47.03715	1.275	47.14577	1.208	47.30045	1.233	76.08252	1.279
47.03990	1.270	47.14852	1.190	47.30320	1.194	76.08527	1.269
47.04265	1.286	47.15127	1.196	47.30595	1.201	76.08803	1.265

of models with assumed values of mass ratio q which is from 0.04 to 1.00. The sums of weighted square deviations $\sum W_i(O-C)_i^2$ for all the assumed values of q are plotted in Figure 4. A minimum value is found at $q = 0.10$. Then, we chose $q = 0.10$ as the initial value and an adjustable parameter and started a differential correction. Finally, the photometric solution is converged at $q = 0.0870$. As seen in the light curve of GSC 02265-01456, a clear O'Connell effect can be found. Therefore, we started the W–D program using a spot model. Extensive study revealed that a dark spot on the primary component leads to the best fit. The determined photometric elements are listed in Table 3. The residual without spot is much bigger than that with spot. Therefore, we chose the dark spot model as the final solution. The mass

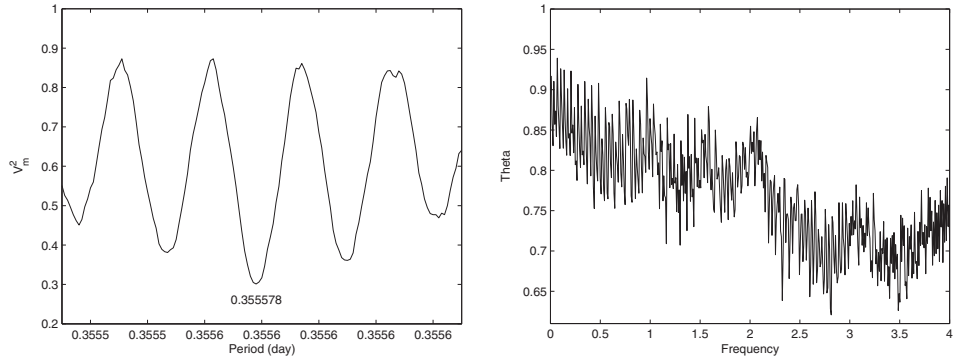

Figure 2. Period analysis using all the V band data spanning six years: the left panel is based on the Jurkevich method, the right panel is derived by the software PDM13.

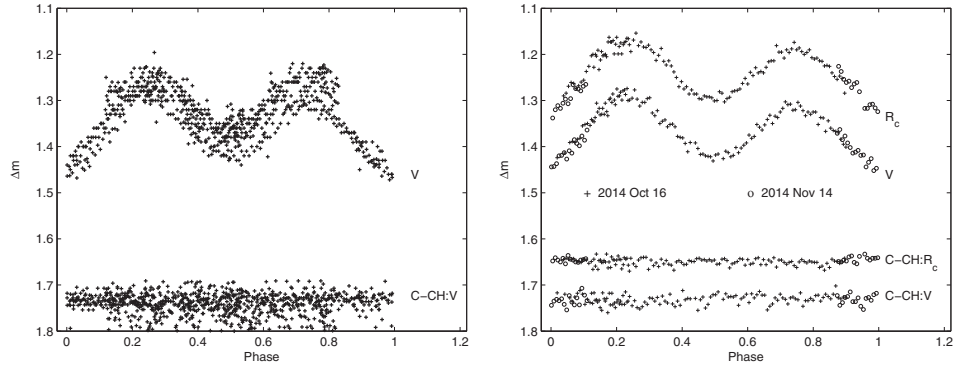

Figure 3. The left panel shows the folded V band light curves of GSC 02265-01456 based on all the data spanning 6 years. The large scatter of the light curve is due to insufficient exposure time or weather conditions. The right panel shows the newly observed V and R_c light curves. The phases were calculated using equation (1). The magnitude differences between the comparison and the check stars are also shown in the figure, whose standard deviations are 0.011 and 0.007 for V and R_c bands, respectively.

ratio determined by considering the dark spot is 0.087, which is a little different from the value without spot. The small difference in the mass ratios is due to the dark spot effect. We also carried out photometric analysis by adding the third light (L3), but the value of L3 is always negative. The theoretical light curves obtained by dark spot model are shown in Figure 5. The geometrical structures of GSC 02265-01456 at phase 0.00 and 0.75 are displayed in Figure 6.

4. Results and conclusion

The V and R_c light curves of a newly identified eclipsing binary GSC 02265-01456 were presented. This binary is very faint ($V = 15.46$ mag). The orbital period of GSC 02265-01456 was determined to be $P = 0.355578$ days, based on Jurkevich method, and confirmed by the software PDM13. The two band light curves

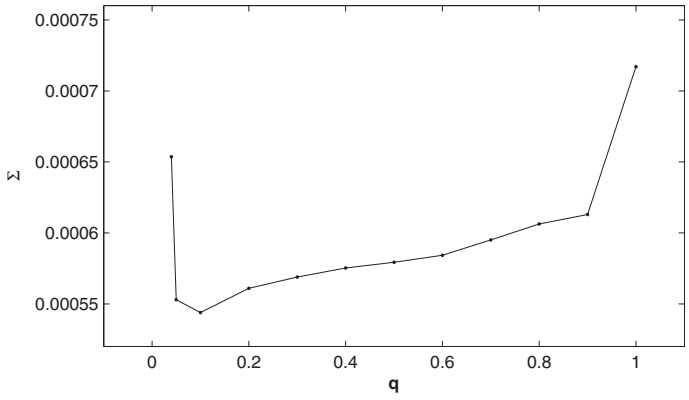

Figure 4. $\sum -q$ relation of GSC 02265-01456.

Table 3. Photometric solutions for GSC 02265-01456.

Parameters	Without spot	Errors	With spot	Errors
$g_1,\ g_2$	1, 0.32	Assumed	1, 0.32	Assumed
$A_1,\ A_2$	1, 0.5	Assumed	1, 0.5	Assumed
$x_{1\mathrm{bol}},\ x_{2\mathrm{bol}}$	0.163, 0.093	Assumed	0.163, 0.082	Assumed
$y_{1\mathrm{bol}},\ y_{2\mathrm{bol}}$	0.558, 0.632	Assumed	0.558, 0.646	Assumed
$x_{1V},\ x_{2V}$	0.031, 0.059	Assumed	0.031, 0.036	Assumed
$y_{1V},\ y_{2V}$	0.764, 0.726	Assumed	0.764, 0.643	Assumed
$x_{1R_c},\ x_{2R_c}$	0.02, −0.024	Assumed	0.02, −0.043	Assumed
$y_{1R_c},\ y_{2R_c}$	0.696, 0.735	Assumed	0.696, 0.745	Assumed
T_1(K)	7900	Assumed	7900	Assumed
$q(M_2/M_1)$	0.080	±0.002	0.087	±0.001
Ω_{in}	1.8953	Assumed	1.9189	Assumed
Ω_{out}	1.8427	Assumed	1.8618	Assumed
T_2(K)	6902	±211	7171	±187
i	54.4	±1.9	53.2	±0.7
L_{1V}/L_V	0.9350	±0.0018	0.9278	±0.0011
L_{1R_c}/L_{R_c}	0.9278	±0.0018	0.9213	±0.0010
$\Omega_1=\Omega_2$	1.8524	±0.0094	1.8670	±0.0091
r_1 (pole)	0.5609	±0.0072	0.5583	±0.0028
r_1 (side)	0.6392	±0.0130	0.6353	±0.0050
r_1 (back)	0.6593	±0.0152	0.6568	±0.0059
r_2 (pole)	0.1947	±0.0153	0.2026	±0.0057
r_2 (side)	0.2051	±0.0188	0.2138	±0.0071
r_2 (back)	0.2716	±0.0910	0.2936	±0.0486
f	81.8%	±11.5%	82.5%	±10.5%
θ (radian)	–	–	1.922	±0.590
ϕ (radian)	–	–	1.221	±0.072
r (radian)	–	–	0.638	±0.086
$T_f(T_d/T_0)$	–	–	0.955	±0.096
$\Sigma W(O-C)^2$	0.00055		0.00033	

were simultaneously analyzed by the W–D code. Photometric solutions show that GSC 02265-01456 is an extremely low mass ratio overcontact binary ($q = 0.087$, $f = 82.5\%$). As shown in the right panel of Figure 2, a clear O'Connell effect can be seen. A dark spot on the primary component was introduced to explain the effect.

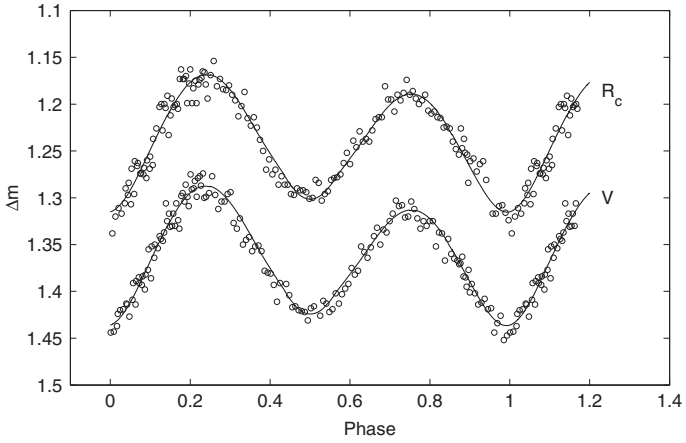

Figure 5. Observed (symbols) and theoretical (lines) light curves in the V and R_c bands for GSC 02265-01456.

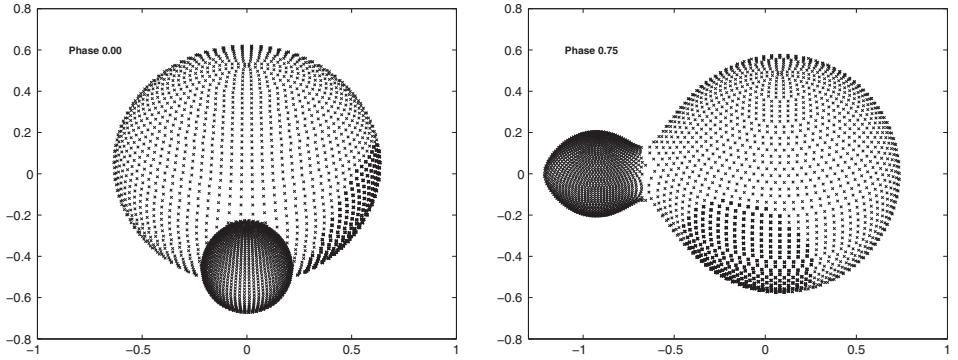

Figure 6. The geometrical structure of the deep, low mass ratio overcontact binary GSC 02265-01456 at phase 0.00 and 0.75.

The absolute dimensions of GSC 02265-01456 can be roughly estimated by employing the following equation (Rucinski & Duerbeck 1997):

$$M_v = -4.44 \log P + 3.02(B - V)_0 + 0.12. \quad (2)$$

After the correction of interstellar extinction, the $(B - V)_0$ of GSC 02265-01456 was derived to be 0.20, and the period is 0.355578. So, employing this equation, we obtain M_v of GSC 02265-01456 to be 2.72 mag. Now taking the visual magnitude (V) as 15.46, the distance modulus of GSC 02265-01456 is calculated to be 12.74 mag, leading to a distance of about 3277.9 pc by considering the extinction correction as $A_V = 0.162$ based on NED. In addition, this distance is the upper limit because the binary star has been considered as a single star.

GSC 02265-01456 is a deep, low mass overcontact binary with a mass ratio of $q = 0.087$ and an overcontact degree of $f = 82.5\%$. This kind of binary, such as V857 Her, $f = 83.8\%$ (Qian *et al.* 2005); QX And, $f = 83.8\%$ (Qian *et al.* 2007);

DN Boo, $f = 64\%$ (Senavci *et al.* 2008), is at the late evolutionary stage and may be going to merge. So, the study of those stars can help us to understand the dynamical evolution of binaries and the formation of blue straggler (BS) and FK Com type stars (Eggleton & Kiseleva-Eggleton 2001). Future observations are required to analyze the evolution of the binary and to investigate the orbital period variations.

Acknowledgements

This work is partly supported by the National Natural Science Foundation of China (Nos 11203016, U1431105), the Natural Science Foundation of Shandong Province (No. ZR2014AQ019), the Basic Research Program of Shandong University at Weihai (No. 2015ZQXM013), and by the Open Research Program of Key Laboratory for the Structure and Evolution of Celestial Objects (No. OP201303). The authors would like to thank the referee for very helpful suggestions and comments.

References

Bonanos, A. Z., Stanek, K. Z., Sasselov, D. D., Mochejska, B. J., Macri, L. M., Kaluzny, J. 2003, *AJ*, **126**, 175.
Cox, A. N., *Allen's astrophysical quantities*, 4th ed., Publisher: New York: AIP Press; Springer (2000)
Eggleton, P. P., Kiseleva-Eggleton, L. 2001, *ApJ*, **562**, 1012.
Guinan, E. F., Ribas, I., Fitzpatrick, E. L., Giménez, Á., Jordi, C., McCook, G. P., Popper, D. M. 2000, *ApJ*, **544**, 409.
Guo, D.-F., Li, K., Hu, S.-M., Jiang, Y.-G., Gao, D.-Y., Chen, X. 2014, *PASJ*, **66**, 100.
Guo, D.-F., Li, K., Hu, S.-M., Jiang, Y.-G., Gao, D.-Y., Chen, X. 2015, *RAA*, **15**, 889.
Hu, S. M., Han, S. H., Guo, D. F., Du, J. J. 2014, *RAA*, **14**, 719.
Jurkevich, I. 1971, *Ap&SS*, **13**, 154.
Kaluzny, J., Thompson, I. B., Rozyczka, M., Dotter, A., Krzeminski, W., Pych, W., Rucinski, S. M., Burley, G. S., Shectman, S. A. 2013, *AJ*, **145**, 43.
Lucy, L. B. 1967, *Z. Astrophys.*, **65**, 89.
North, P., Gauderon, R., Barblan, F., Royer, F. 2010, *A&A*, **520**, 74.
Pols, O. R., Tout, C. A., Schroder, K., Eggleton, P. P., Manners, J. 1997, *MNRAS*, **289**, 869.
Qian, S.-B., Liu, L., Soonthornthum, B., Zhu, L.-Y., He, J.-J. 2007, *AJ*, **134**, 1475.
Qian, S.-B., Zhu, L.-Y., Soonthornthum, B., Yuan, J.-Z., Yang, Y.-G., He, J.-J. 2005, *AJ*, **130**, 1206.
Ruciński, S. M. 1969, *Acta Astronomica*, **19**, 245.
Rucinski, S. M., Duerbeck, H. W. 1997, *PASP*, **109**, 1340.
Senavci, H. V., Nelson, R. H., Özavcı, İ., Selam, S. O., Albayrak, B. 2008, *NewA*, **13**, 468.
Schlafly, E. F., Finkbeiner, D. P. 2011, *ApJ*, **737**, 103.
Torres, G., Ribas, I. 2002, *ApJ*, **567**, 1140.
Van Hamme, W. 1993, *AJ*, **106**, 2096.
Wilson, R. E. 1990, *ApJ*, **356**, 613.
Wilson, R. E. 1994, *PASP*, **106**, 921.
Wilson, R. E., Devinney, E. J. 1971, *ApJ*, **166**, 605.
Zacharias, N., Monet, D. G., Levine, S. E., Urban, S. E., Gaume, R., Wycoff, G. L. 2004, *AAS*, **205**, 4815.
Zalian, C., Chadid, M., Stellingwerf, R. F. 2014, *MNRAS*, **440**, 68.